Strongly Enhanced Antibacterial Action of Copper Oxide Nanoparticles with Boronic Acid Surface Functionality

Ahmed F. Halbus,[a,b] Tommy S. Horozov,[a] Vesselin N. Paunov[a]*

[a] Department of Chemistry and Biochemistry, University of Hull, Hull, UK;

[b] Department of Chemistry, College of Science, University of Babylon, Hilla, IRAQ.

KEYWORDS CuONPs; copper oxide, antibacterial nanoparticles, E. coli, R. rhodochrous, 4-Hydroxyphenylboronic acid; boronic acid, sugar, carbohydrates.

ABSTRACT: Copper oxide nanoparticles (CuONPs) have been widely recognized as good antimicrobial agents but are heavily regulated due to environmental concerns of their post use. In this work, we have developed and tested a novel type of formulation for copper oxide (CuONPs) which have been functionalized with (3-Glycidyloxypropyl)trimethoxysilane (GLYMO) to allow further covalent coupling of 4-Hydroxyphenylboronic acid (4-HPBA). As the boronic acid (BA) groups on the surface of CuONPs/GLYMO/4-HPBA can form reversible covalent bonds with the diols groups of glycoproteins on the bacterial cell surface, they can strongly bind to the cells walls resulting in a very strong enhancement of their antibacterial action which is not based on electrostatic adhesion. SEM and TEM imaging revealed that 4-HPBA-functionalized nanoparticles could accumulate more on the cell surface than non-functionalized ones. We demonstrate that the CuONPs with boronic acid surface functionality are far superior antibacterial agents compared to bare CuONPs. Our results showed that, the antibacterial impact of the 4-HPBA functionalized CuONPs on *Rhodococcus rhodochrous* (*R. rhodochrous*) and *Escherichia coli* (*E.coli*) is one order of magnitude higher than that of bare CuONPs or CuONPs/GLYMO. We also observed a marked increase of the 4-HPBA functionalized CuONPs antibacterial action on these microorganisms at shorter incubation times compared with the bare CuONPs at the same conditions. Significantly, we show that the cytotoxicity of CuONPs functionalized with 4-HPBA as an outer layer can be controlled by the concentration of glucose in the media and that the effect is reversible as glucose competes with the sugar residues on the bacterial cell walls for the BA-groups on the CuONPs. Our experiments with human keratinocyte cell line exposure to CuONPs/GLYMO/4-HPBA indicated lack of measurable cytotoxicity at particle concentration which are effective as antibacterial agent for both *R. rhodochrous* and *E.coli*. We envisage that formulations of CuONPs/GLYMO/4-HPBA can be used to drastically reduce the overall CuO concentration in antimicrobial formulations while strongly increasing their efficiency.

INTRODUCTION

Spreading of antimicrobial resistance among common bacterial pathogens, bacterial infections, including antibiotic-resistant infections, have recently drawn much attention.[1] A range of colloidal particles are being extensively studied in various antimicrobial applications due to their small size to volume ratio and ability to exhibit a wide spectrum of antibacterial action.[2-5] Antibacterial NPs could bypass the increasing rates of antibiotic resistance by attacking and destroying the bacteria in other ways.[6] Surface functionalization of nanoparticles is vital for controlling their properties and interactions with molecules and ligands of relevance for biomedical applications, in addition to their susceptibility to undergo a transformation in environmental and biological systems.[45,46] Considerable efforts have been devoted to the development of surface modifiers that can offer not only stability but also better control of the interaction between nanoparticles and biological membranes in order to obtain more biocompatible materials.[47] For example, Al-Awady *et al.*[44] produced polyelectrolyte-coated titania nanoparticles with up to 4 layers of polyelectrolytes of alternating charge (PSS and PAH) using the layer-by-layer technique. They showed that the antimicrobial properties of polyelectrolyte-coated nanoparticles alternate with the surface charge for the particles with cationic outer layer (or bare nanoparticles) being much more effective antimicrobials than the ones with an outer layer of anionic polyelectrolyte. The anionic nanoparticles (NPs/PSS and NPs/PSS/PAH/PSS) showed much lower activity towards than the cationic ones, NPs/PSS/PAH and the bare NPs, respectively. These authors suggested that the decrease of antimicrobial action can be explained by the poor adhesion of the anionic nanoparticles (NPs/PSS and NPs/PSS/PAH/PSS) to the cell walls due to their electrostatic repulsion. In contrary, the enhancement of the antimicrobial effect for cationic nanoparticles (bare NPs and NPs/PSS/PAH) is due to the amplification of the particle-cell electrostatically driven adhesion.[2,35] Perreault and co-workers have exhibited that polymer coated (polystyrene-co-butyl

acrylate) CuONPs showed increased cellular uptake and toxicity in the green alga *C. reinhardtii*. The ascorbate and citrate surface layers are well known for their anti-oxidant properties and are used as reducing agents as well as negatively charged stabilizers of nanoparticles synthesis and dispersion.[48]

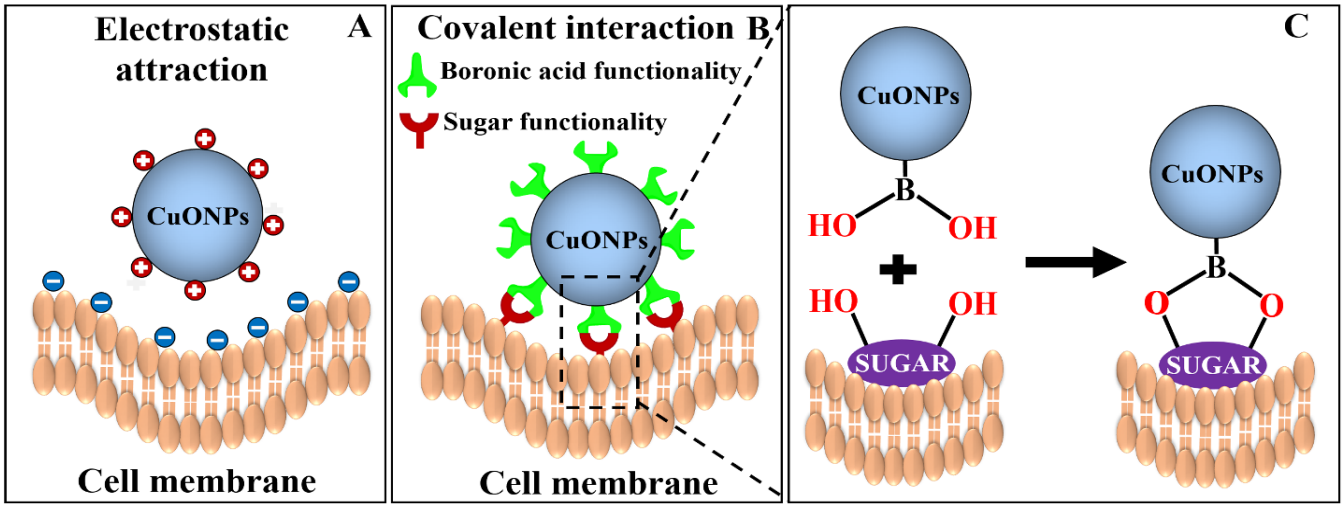

Figure 1. The perceived attachment mechanisms of CuONPs to the bacterial cell membranes. (A) Electrostatic attraction between bare CuONPs and the cells; (B) covalent bonding between CuONPs/GLYMO/4-HPBA and the cells. (C) The interaction between the CuONPs with boronic acid surface functionality and the sugar groups on the surface of the bacterial cell wall.

Líbalová *et al*. have evaluated the cytotoxicity of a panel of CuONPs with various surface modifications such as cationic polyethylenimine (PEI), neutral polyvinylpyrrolidone (PVP), sodium ascorbate (ASC) and anionic sodium citrate (CIT), versus the pristine bare CuONPs, using a murine macrophage cell line. The results from their work suggest that the PEI-coated CuONPs were found to be the most cytotoxic. Líbalová *et al*. have also reported that the ascorbate-coated CuONPs, which were found to be the least cytotoxic, produced lower levels of ROS in comparison to bare nanoparticles.[46]

CuONPs have been widely used as a dopant for semiconductors, chemical sensors, supported heterogeneous nano-catalysts, coating material and in anti-cancer treatments but their functional properties have been proven essential for their applications in biological research.[7,8] Lazary and co-workers have stated that CuONPs have been widely used in hospitals as anti-microbial agents due to their ability to kill more than 99.9% of both Gram-negative and Gram-positive bacteria within 2 hours of treatment of various surfaces. It has been found that the use of CuO in this way has radically decreased the occurrence of hospital-acquired infections and the costs associated with health care. A non-intravenous approach to utilizing CuONPs in bed sheets is a very exciting innovation as the particles can decrease microbial attachment and therefore limit hospital acquired infections.[9] By synthesizing a hybrid inorganic/organic species in the form of a Cu-chitosan nanoparticle, Usman *et al.*[10] have found that their antimicrobial action is highly effective when the coated particles have a size range of 2–350 nm. The same research team has evaluated the antibacterial and antifungal activities of these nanoparticles on different microorganisms, including methicillin-resistant *Staphylococcus aureus*, *Salmonella choleraesuis*, *Candida albicans*, *Pseudomonas aeruginosa*, and *Bacillus subtilis*. The results from their work have shown that the highly effective Cu-chitosan particles are very active as antimicrobial agents in anaerobic conditions. Note that Cu nanoparticles have the ability to rapidly oxidize, which limits their applications as antimicrobials when used in aerobic conditions.[10,11] Katwal and others have developed a new CuONPs preparation route by using electrochemical methods and demonstrated that they can control the CuONPs morphologies. [12] CuO particles can be produced in various shapes and sizes, and can provide enhanced antibacterial activity against several pathogenic strains. Mahapatra *et al.*[11] tested the antibacterial action of CuONPs towards *Klebsiella pneumoniae*, *Salmonella paratyphi*, *Shigella strains* and *Pseudomonas aeruginosa* and showed that the nanoparticles have been efficient against these bacteria. They envisaged that CuONPs can cross through the bacterial cell membrane and affect vital enzymes in the bacteria cytoplasm leading to their death. It has also been shown that CuONPs are not cytotoxic on some human cells (e.g. HeLa cell line). Azam *et al.* [13] have also reported that the activity of CuO based nanoparticles is dependent on their particle size when used as an antibacterial agent. In their study, they examined two Gram-negative bacteria (*E. coli* and *P. aeruginosa*) and two Gram-positive bacteria (*B. subtilis* and *S. aureus*). It was found that CuONPs exhibited inhibitory effects towards both groups of bacteria, which clearly depended on their stability, particle size and concentration when incubated with the bacterial culture. They concluded that the CuONPs can limit the bacterial growth by interacting with nanometric pores that exist on the cell membranes of most microorganisms. Ahamed and co-workers discovered that CuONPs with a size of ~23 nm had significant

antimicrobial action towards various bacterial strains (*Klebsiella pneumoniae*, *Pseudomonas aeruginosa*, *Escherichia coli*, *Enterococcus faecalis*, *Shigella flexneri*, *Salmonella typhimurium*, *Staphylococcus aureus*, and *Proteus vulgaris*). *Escherichia coli* and *Enterococcus faecalis* showed the highest sensitivity to CuONPs while *Klebsiella pneumoniae* was resistant to this treatment.[2,7,8] Note that the bare CuONPs are cationic at neutral pH and can adhere to the negatively charged bacterial cell walls only by electrostatic interactions.

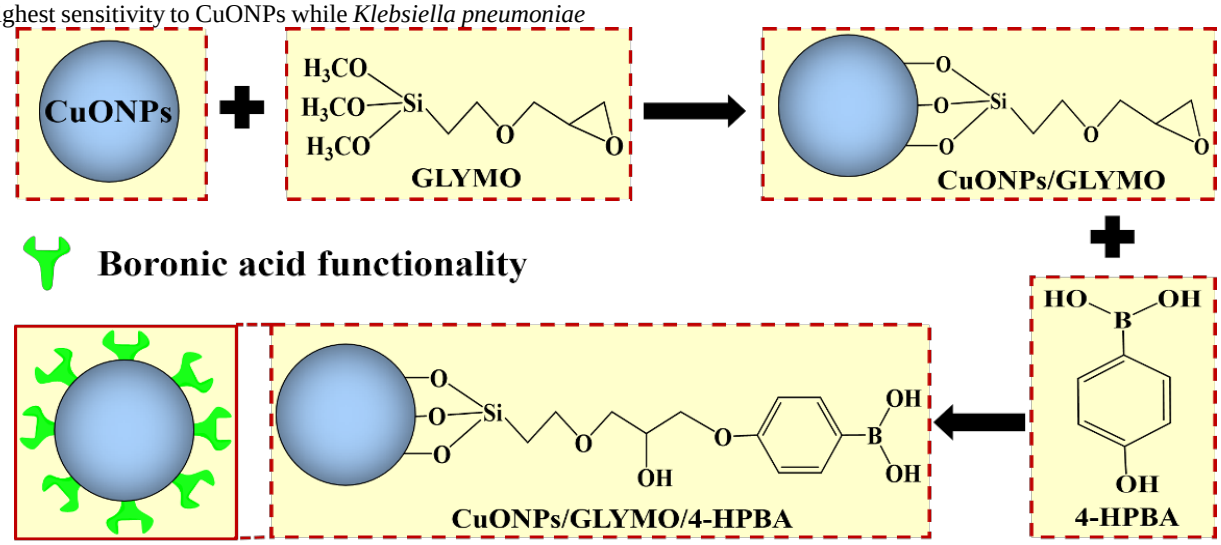

Figure 2. The schematic of the surface functionalization of CuONPs with GLYMO and 4-HPBA.

The average size of CuONPs is also essential for their potential antimicrobial activity, as smaller nanoparticles have higher portability and ability to potentially penetrate and relocate between the bacterial cell compartments. This makes them very effective antimicrobial agents. However, electrostatic adhesion can be easily disabled by the presence of another type of anionic substances in the solution, e.g. organic acids, albumins, surfactants, polymers and others. It impacts the nanoparticle interactions with different biomolecules, for example, carbohydrates and proteins which can be adsorbed on the particles and form a corona of different surface properties to that of the original nanoparticles. This is the likely reason why CuONPs can quickly lose their antimicrobial activity in biological fluids as well as in formulations that contain anionic polyelectrolytes and surfactants.

Here we engineered CuONPs with boronic acid surface functionality in an attempt to design a non-electrostatic mechanism for their attachment to the bacteria which was expected to amplify their accumulation on the cell walls despite the presence of other anionic species. This is shown schematically in Figure 1. Our idea here is to introduce boronic acid (BA) surface groups on the CuONPs which are able to covalently bind to various glycoproteins and carbohydrates that are abundant on the bacterial cell walls.

Boronic acid has been used before in chemosensor applications due to its high sensitivity for sugar determination.[14] An attractive feature of the BA surface functionality that makes it very effective for biomedical applications is their perceived absence of toxicity[15] despite its ability to form reversible covalent complexes with diols.[16,17] The binding of BA to sugars is very sensitive to the sugar concentration, however, it is undiscriminating and will therefore bind to any diol containing compounds.[18] BA has also been discussed as a promising tools for the quantification of the total content of bacteria.[19-21] BA surface groups can covalently bind to saccharides and form boronic esters.[22-24]

We used *R. rhodochrous* and *E.coli* as model bacteria species to examine the antibacterial activity of the 4-HPBA functionalized CuONPs. The current work was carried out with CuONPs, CuONPs/GLYMO and CuONPs/GLYMO/4-HPBA to investigate the impact of (i) the nanoparticle concentration, and (ii) the zeta potential and particle size on the viability of *R. rhodochrous* and *E.coli* at different exposure times. The novelty of our work is that the antibacterial activity of CuONPs functionalized with 4-HPBA is not based on electrostatic adhesion to the bacterial cells and therefore could potentially be used in complex biological environment. Significantly, the functionalization of the CuONPs with 4-HPBA groups as an outer monolayer should lead to their covalent attachment on the sugar (OH) groups on the membrane surface, thus bringing the CuONPs in very close proximity to the bacterial cell membrane and increasing their efficiency (Figure 1B and 1C). We also examined the toxicity of both bare CuONPs and functionalized CuONPs on human keratinocytes.

MATERIALS AND METHODS

Materials

We used copper (II) chloride (99%, Sigma Aldrich) as a precursor in the synthesis of CuONPs by the direct precipitation method. Sodium hydroxide (99.6%, Fisher, UK) was used as a precipitating agent to synthesise CuONPs. (3-glycidyloxypropyl) trimethoxysilane (GLYMO) and 4-hydroxyphenylboronic acid (4-HPBA) were purchased from Sigma Aldrich. BacTiter-Glo (BTG) microbial cell viability assay was delivered by Promega, UK. *Escherichia coli*, sourced

from Thermofisher (Invitrogen MAX Efficiency™ DH10B™) was kindly provided for our antibacterial tests by Prof J. Rotchell's group at the University of Hull, UK. *R. rhodochrous* was supplied by Blades Biological Ltd., UK. Deionized water purified by reverse osmosis and ion exchange with a Milli-Q water system (Millipore, UK) was used in all our studies. Its surface tension was 71.9 mNm^{-1} at 25°C, with measured resistivity more than 18 MΩ cm^{-1}.

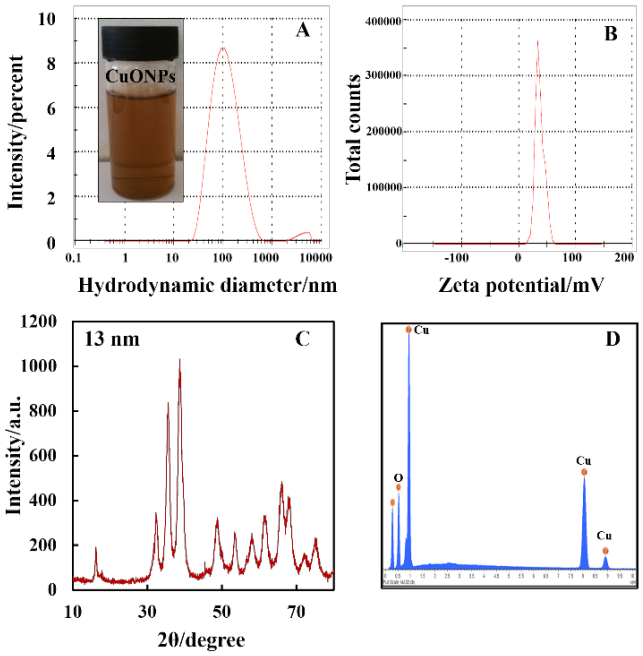

Figure 3. Plots of (A) particle size and (B) zeta potential distribution of CuONPs produced by annealing at 100 °C. The size and zeta potential of CuONPs was measured utilizing the Malvern Zetasizer Nano ZL at room temperature with the average data of three runs. (C) XRD pattern of CuONPs annealed at 100 °C. The largest peak in the XRD results was used to determine the crystallite size. (D) EDX spectrum of CuONPs.

Methods

Synthesis of CuONPs. In first stage of the preparation, 3.0 g of copper (II) chloride ($CuCl_2$) was dissolved in 160 mL of ethanol. 1.8 g of sodium hydroxide (NaOH) was dissolved in 50 mL ethanol. The NaOH solution was added dropwise to $CuCl_2$ solution under constant stirring at room temperature. During the course of the reaction, the color of the solution turned from green to greenish blue and lastly to black. This black precipitate was copper hydroxide, $Cu(OH)_2$ (see Figure S1) which was centrifuged, washed with ethanol and deionized water, and dried at 60 °C in the electric furnace. In order to produce CuONPs, the sample of dry $Cu(OH)_2$ was annealed at different temperatures, 100 °C, 200 °C, 300 °C, 400 °C, 500 °C and 600 °C (see Figures S2 and S3) followed by grinding to obtain CuO in powdered form.[25] CuONPs were produced by dispersing CuO in Milli-Q water at pH 6 via a sonication (Branson 450, 5 mm tip, 400 W maximum power) at 40% of the maximum power for 10 minutes (2 s ON - 2 s OFF pulse time).

Surface Functionalization of CuONPs by GLYMO and 4-HPBA. A sample of 0.1 g of CuONPs was dispersed into deionized water (100 mL, pH 6–6.5). The suspension was stirred for 1 hour and 0.1 wt% of GLYMO were added. The reaction mixture was stirred for a further 24 hours, then the unreacted GLYMO was removed by centrifugation and washing with deionized water three times. The process is analogous to the APTES functionalization of other inorganic nanoparticles[26] but in our case GLYMO brings epoxy-ring as a terminal group. This functionality has not been reported before for CuONPs. The GLYMO- functionalized CuONPs pellet was then re-dispersed in 100 mL of deionized water and mixed drop-wise with 0.1 g of 4-HPBA dissolved in 100 mL of ethanol solution. The mixture was shaken for 2 hours, then washed and centrifuged three times with ethanol at 10000 rpm for 30 minutes. The CuONPs/GLYMO/4-HPBA produced were finally re-dispersed in 100 mL of deionized water.[27-29] The chemistry of the process of surface functionalization of CuONPs with phenyl boronic acid is shown in Figure 2.

Characterization of the Surface Functionalized CuONPs. The particle size and the zeta potential of the surface functionalized CuONPs (with GLYMO and 4-HPBA) was examined by dynamic light scattering (DLS) using the Malvern Zetasizer Nano ZL instrument. The zeta potential values of the surface functionalized CuONPs were determined after dispersing the CuONPs samples in deionized water using an ultrasonic probe. After that, a range of CuONPs suspensions with pH from 3 to 12 was made by using 0.1 M HCl and 0.1 M NaOH and adding two drops of 0.01 M NaCl into each sample (10 mL). All measurements have been done at room temperature and the results reported are an average of 3 runs.

Antibacterial Activity of Bare and Surface Functionalized CuONPs on *E. coli* and *R. rhodochrous*. 10 mL of the bacteria culture was centrifuged and washed three times with deionized water for 4 minutes at 4000 rpm, and re-dispersed in 100 mL deionized water. Then, 5 mL of the washed bacteria were incubated with a series of 5 mL aliquots of the CuONPs suspension at various particles concentrations. The number of bacteria was measured directly after removing the excess nanoparticles from the bacteria dispersion. Then, 1 mL of each bacteria suspension was washed and re-suspended in 1 mL deionized water. 100 µL aliquot of the washed bacteria suspension was then incubated with 100 µL of BTG reagent in a white opaque 96-well microplate with solid flat bottom, and after that shaken for 30 seconds, and incubated at 30 °C for 5 minutes. The relative luminance was measured as a function of the incubation time and used to calculate the fraction of viable bacteria upon exposure to various concentrations of CuONPs. We did the same experiments with CuONPs functionalized with GLYMO as well as ones functionalized with GLYMO and 4-HPBA at various particle concentrations.

Colony Forming Units assessment for antimicrobial assay. The bacteria were grown overnight in sterilized LB medium at 37 °C to produce viable colonies. Bacterial cells were pelleted down by centrifugation at 5000 rpm for 10 minutes followed by washing (twice) with 0.85 w/v% serial saline until an optical density of 0.08-0.12 at 625 nm was obtained using a spectrophotometer. These adjusted bacterial saline suspensions were then diluted 1:150 into LB to yield

starting concentrations between $5 \times 10^5 - 1 \times 10^6$ colony forming units per mL (CFU/mL). Then flasks 250 mL containing LB medium 100 mL with different concentrations of the bare CuONPs and surface functionalized of CuONPs with GLYMO and 4-HPBA were inoculated with an equal volume of the bacterial suspension. Flasks containing bacterial cells and media without nanoparticles were used as control. All the flasks were incubated for 10 min, 1 hour and 6 hours in a shaker at 37 ^oC with 140 rpm. After that, the serial dilutions were made of all the treated samples including control and 100 µL of each were homogeneously spread on LB agar plates for colony forming unit (CFU). The growth rate of bacterial cells interacting with the nanoparticles was determined from a plot of the CFU/mL versus concentrations. The time-kill assay was repeated in three independent experiments

Zeta Potential Measurements of *E.coli* after Treatment with CuONPs. The changes in the surface charge of the bacteria after incubation with the bare and the surface modified CuONPs were determined by a Zetasizer nano ZL instrument (Malvern, UK) at nanoparticle concentrations of 0, 5, 10, 15, 20, and 25 µg mL^{-1}. Equal aliquots of the cell culture was used to measure the average zeta potential value of the bacteria after being incubated with the particles. All measurements were done in triplicates.

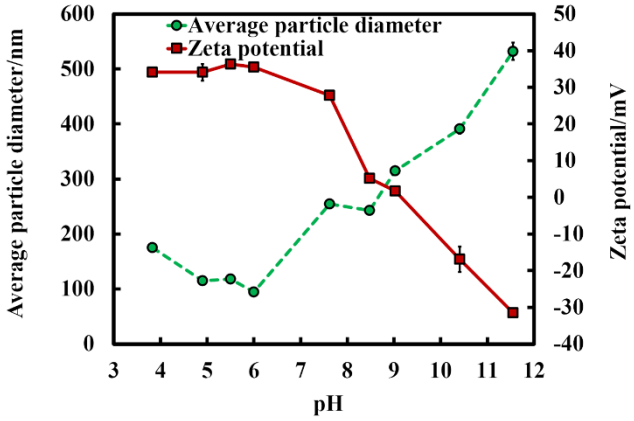

Figure 4. Zeta potential and particle diameter of bare CuONPs versus pH of the aqueous suspension.

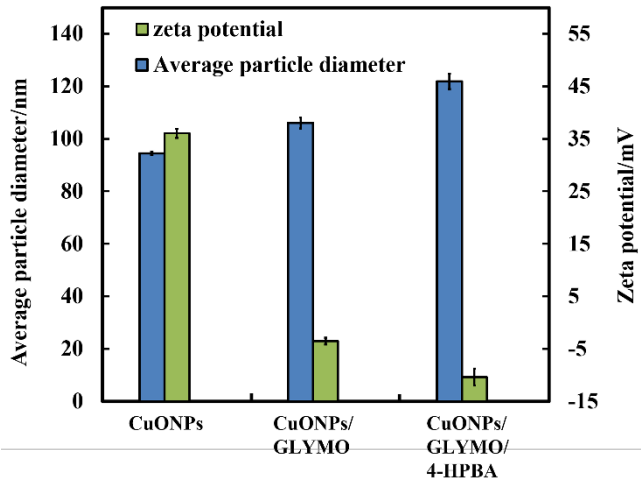

Figure 5. Zeta potential and hydrodynamic diameter of the bare and surface modified CuONPs with GLYMO and 4-HPBA, measured at room temperature at pH 6 (error bars are standard deviations).

SEM and TEM Sample Preparation Protocol for *E.coli* and *R. rhodochrous* after Exposure to HPBA-Functionalized CuONPs. After incubation with the HPBA-surface modified CuONPs, the *E.coli* and *R. rhodochrous* were fixed with 2.5% glutaraldehyde at room temperature for two hours in 0.1M cacodylate buffer pH 7.2. These samples were then post-fixed in 1% osmium tetroxide for one hour, and dehydrated in a range of ethanol-water mixtures with increasing ethanol content from 50 vol% up to 100 vol% followed by critical point drying. After incubation with CuONPs, the bacterial cells were prepared for TEM imaging using the following procedure. The bacteria were washed with deionized water to remove the excess of CuONPs at 500 rpm and then fixed in 2 wt% glutaraldehyde for one hour at room temperature followed by treatment with 1 wt% osmium tetroxide for one hour. Then, the samples were incubated for one hour with 2.5 % uranyl acetate and washed with aqueous ethanol solutions of increasing concentration, as described above.

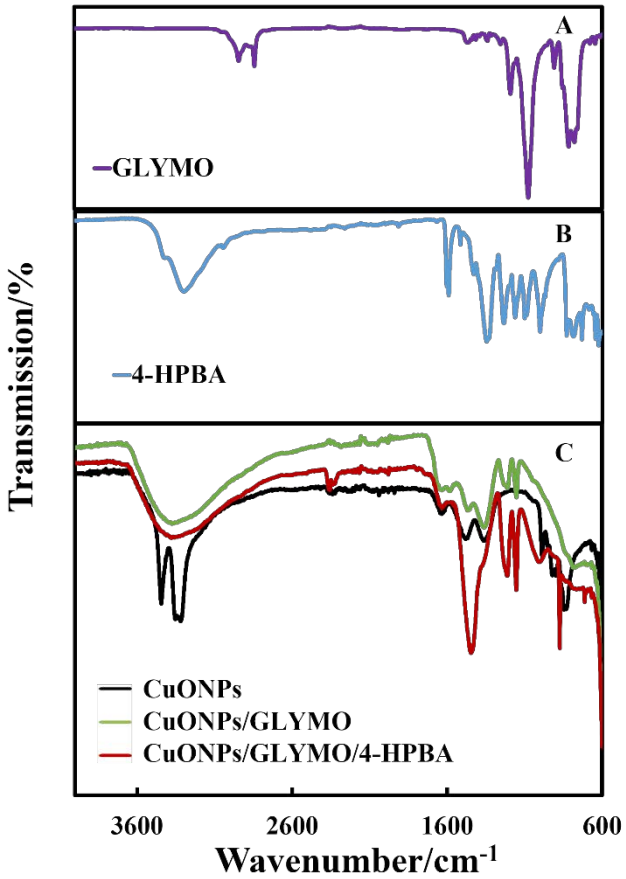

Figure 6. The FTIR spectra of (A) pure GLYMO, (B) pure 4-HPBA and (C) the bare and functionalized CuONPs.

After standard dehydration, the bacterial samples were embedded in fresh epoxy/Araldite at 60 ºC for 2 days, left for 2 days at room temperature and sectioned with an ultra-microtome. Bacteria samples before and after the nanoparticle treatment were imaged by SEM and TEM.

Cytotoxicity Assay of Bare and Surface Functionalized CuONPs on HaCaT Cells.

HaCaT cell line culture (immortalized human keratinocytes) was kindly provided by the Skin Research Group at St James University Hospital at Leeds. The cells were cultured in high-glucose DMEM media supplemented with 10% Fetal Bovine Serum (FBS, Labtech, UK) and 1% antibiotics (Penicillin Streptomycin, Lonza, UK) and placed in an incubator (37°C, 5% CO_2). After reaching 70% confluence, HaCaT cells were carefully washed with PBS for 10 seconds then incubated with 0.25% Trypsin-EDTA (1X, Lonza, UK) to detach the cells from their support after 5 minutes. Its action was neutralized by adding complete DMEM medium before a centrifugation at 400×g for 4 minutes. An 25 mL aliquot of the HaCaT cells culture (~75000 cells mL^{-1}) were washed three times from the culture media via centrifuged, and re-dispersed with 25 mL PBS. Then, 2.5 mL aliquots of this HaCaT cells suspension were incubated with a series of 2.5 mL aliquots of aqueous dispersions of bare and surface functionalized CuONPs at different concentrations. Likewise, a control sample of the HaCaT cells was treated at the similar conditions without exposure to any nanoparticles. After that, 1 mL of the solution HaCaT was taken from each addressed sample with nanoparticles, washed with PBS to remove the excess of nanoparticles via centrifuged at 400×g for 4 minutes. The HaCaT was re-suspended in 1 mL of PBS, then two drops of FDA solution in acetone was added to each sample and mixed together for 15 minutes followed by triple washing with PBS by centrifugation at 400×g for 4 minutes. Finally, a microplate reader was utilized to assay the HaCaT cell viability.

RESULTS AND DISCUSSION

Characterization of CuONPs. We studied the mean particle hydrodynamic diameter and zeta potential of bare and functionalized CuONPs. The results for the non-functionalized particles are presented in Figures S4 and S5 (ESI). The bare CuONPs average particle hydrodynamic diameter was about 93 nm while their average zeta potential was around +37 mV, i.e. the non-functionalized (bare) CuO nanoparticles are cationic at pH 6 (see Figures 3A and 3B). Since the CuONPs are photoactive, there was a concern that the GLYMO/HPBA functionality can potentially be affected by oxidation under the action of UV light. In order to check the stability of this coating against oxidation, we measured periodically the zeta potential of the CuONPs/GLYMO/4-HPBA over the course of 3 days while the samples were exposed to UV light.

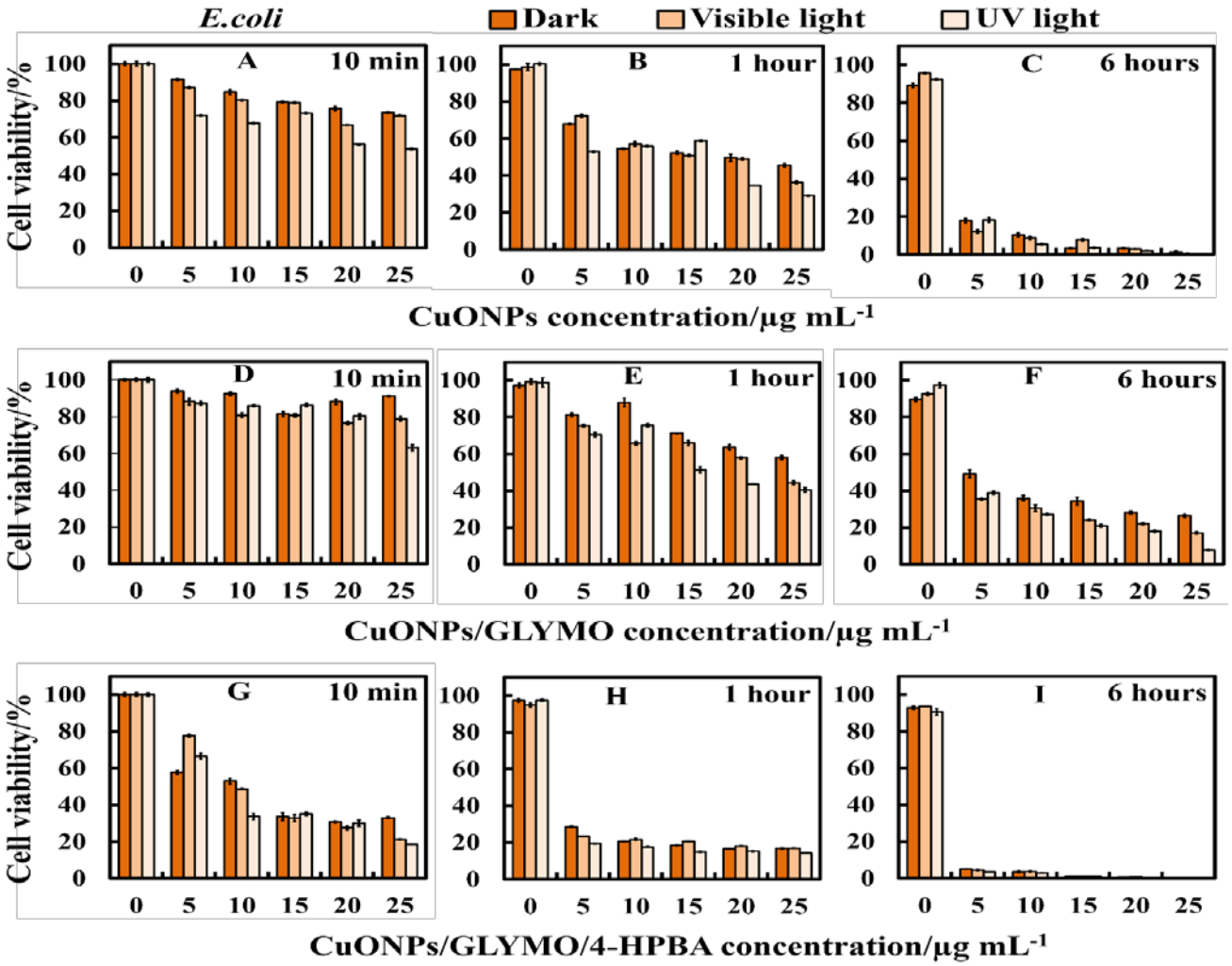

Figure 7. Comparison of the *E.coli* viability at various concentrations of the bare CuONPs (A - C), and surface functionalized of CuONPs with GLYMO (D - F) and 4-HPBA (G - I) in dark, visible and UV light conditions at different incubation times (shown).

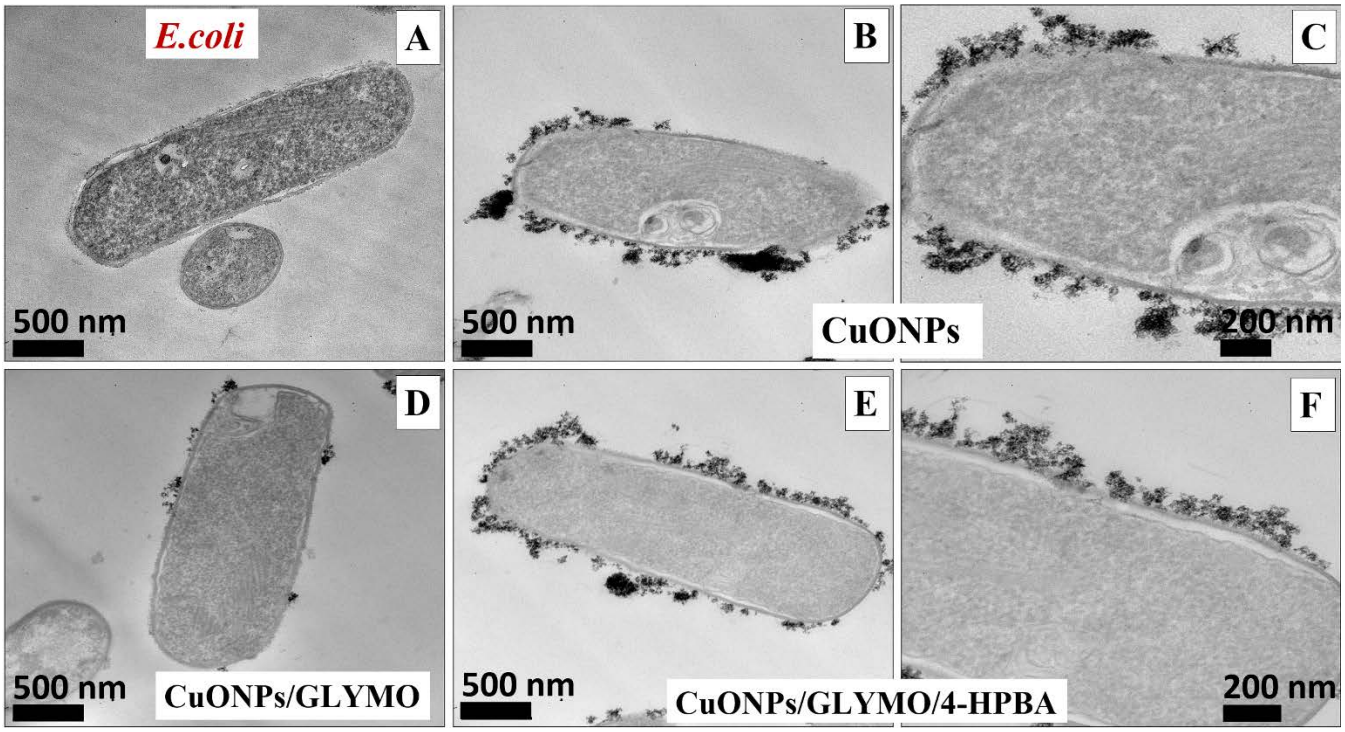

Figure 8. TEM images of *E.coli* at different magnifications: (A) before treatment, and (B, C) after treatment with 25 μg mL^{-1} bare CuONPs, (D) 25 μg mL^{-1} CuONPs/GLYMO and (E, F) 25 μg mL^{-1} CuONPs/GLYMO/4-HPBA, all for 6 hours.

The results, presented in Figure S7 (ESI) indicate that the zeta-potential of the functionalized CuONPs does not change, i.e. the coating is not prone to oxidation at these conditions and hence the particles preserve their functionality and antibacterial action. Figure 3C shows XRD pattern of CuONPs produced by the direct precipitation method and calcinated at 100 °C. The diffraction peaks agree very well with the hexagonal structure of CuO according to the Joint Committee on Powder Diffraction Standards (JCPDS no.01-077-7716). No apparent impurities were detected, suggesting that CuONPs of high purity were prepared. The average crystal size of CuONPs calculated from XRD data using the Scherrer equation was about 13 nm, i.e. much smaller than the hydrodynamic diameters of the CuONPs dispersed in deionized water. This indicates that the CuONPs in aqueous dispersions are aggregates of smaller crystallites. Figure 3D shows the EDX spectrum of CuONPs annealed at 100 °C. The results confirm the presence of only copper (Cu) and oxygen (O) in the CuONPs samples and the data indicate that the nanoparticles were nearly stoichiometric with 73.3 wt % Cu (0.804 keV) and 13.7 wt % O (0.525 keV), respectively. There was no indication of any other elemental impurities in the EDX spectra, i.e. the copper-to-oxygen atomic ratio was 1:1 in the CuONPs, which is in agreement with the literature.[30,31]

Characterization of the CuONPs Surface Functionalized of with GLYMO and 4-HPBA. The zeta potential of bare CuONPs as a function of pH is shown in Figure 4. The isoelectric point (IEP) of the CuONPs (corresponding to the pH where the CuONPs have zero zeta potential) is at pH 9. We found that at pH values above the IEP, the CuONPs partially lost their colloid stability and formed larger aggregates (500 nm or bigger). To avoid the ambiguity related to the particle surface charge being influenced by pH, we carried the antibacterial tests at pH between 5 and 6 (away from the IEP) to ensure that the particle size is around 100 nm. The zeta potentials and hydrodynamic diameters of bare and functionalized CuONPs determined at pH 6 are compared in Figure 5. One can see that the bare CuONPs dispersed in deionized water have the smallest hydrodynamic diameter (94±3 nm), while the diameter of surface-modified CuONPs varied between 106±6 nm (for CuONPs/GLYMO) and 121±4 nm (for CuONPs/GLYMO/4-HPBA).The zeta potential of bare CuONPs was positive while the two types of surface-modified CuONPs had small but negative zeta potential, ranging from around -3±2 mV (CuONPs/GLYMO) to -10±2 mV (CuONPs/GLYMO/4-HPBA) (see Figure 5). The efficiency of the alkoxysilane-mediated functionalization with GLYMO (and latter with 4-HPBA) on CuONPs was examined by FTIR. The OH groups on the surface of the CuO nanoparticles are the reactive sites for the reaction with alkoxy silane groups of GLYMO. Figures 6A, 6B and 6C show normalized FTIR spectra of the bare CuONPs and those, surface modified with GLYMO or GLYMO/4-HPBA. In the spectra of all CuONPs, the broad band between 400 and 800 cm^{-1} corresponds to Cu-O-Cu. GLYMO contains two functional groups: epoxy and methoxysilyl, which can both hydrolyze and condensate. One can see that the epoxy band in FTIR spectra (Figure 6A) is preserved, while the intensity of Si-O-Me band is decreased. Moreover, the two bands of OH groups appear at ~3300 and ~1640 cm^{-1} because of the hydrolysis of Si-O-Me groups.

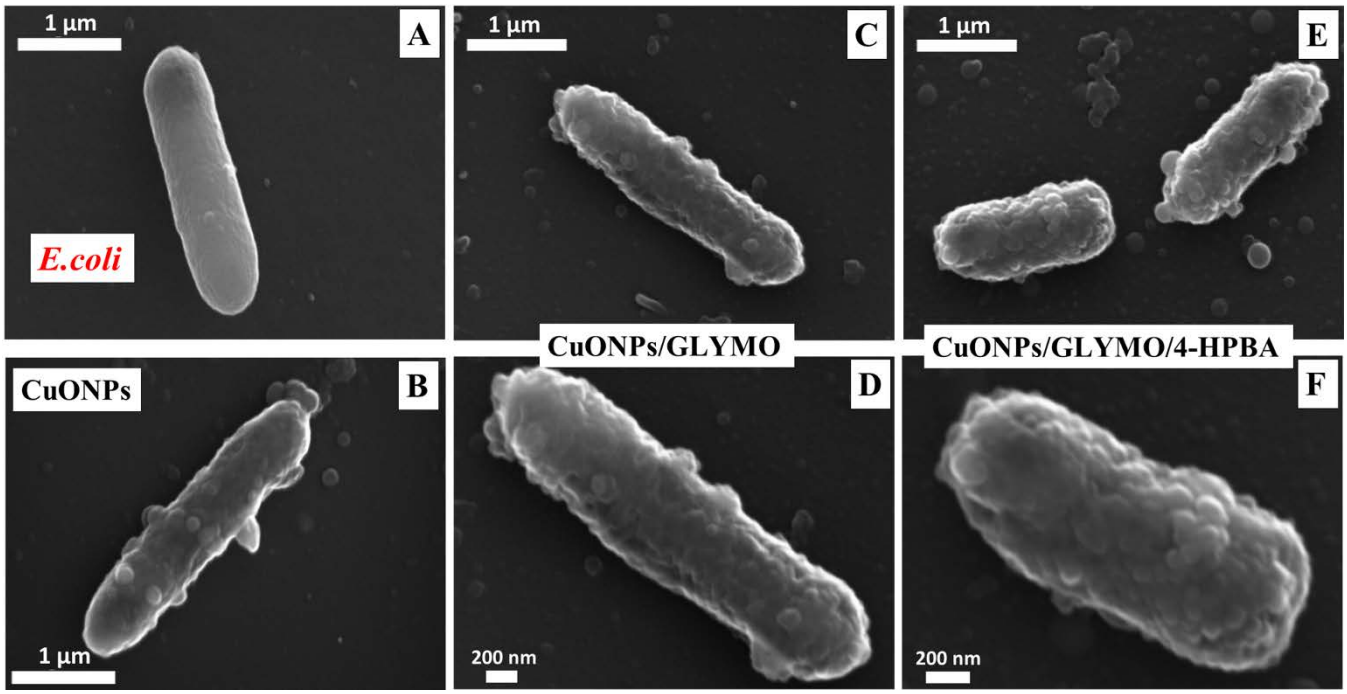

Figure 9. SEM images of *E.coli* after being incubated for 6 hours with bare CuONPs and CuONPs functionalized with GLYMO or 4-HPBA: (A) *E.coli* before treatment, (B) *E.coli* incubated with 25 µg mL^{-1} CuONPs, (C and D) *E.coli* incubated with 25 µg mL^{-1} CuONPs/ GLYMO at different magnifications. (E and F) *E.coli* incubated with 25 µg mL^{-1} CuONPs/GLYMO/4-HPBA at different magnifications. Note the extensive build-up of (B) CuONPs and (E,F) CuONPs/GLYMO/4-HPBA on the *E. coli* cell walls.

Also a peak at 1050 cm^{-1} appears, which can be assigned to the formation of Si-O-Si groups. The comparison of the FTIR spectra of the bare and functionalized CuONPs samples show some new characteristic absorption peaks.

Figure 6C (CuONPs/GLYMO) shows a peak at ~1200 cm^{-1} which refers to Si-O-Me groups.[32] In the FTIR spectrum of the CuONPs/GLYMO/4-HPBA, the peak at about 3300 cm^{-1} could be attributed to the stretching vibration of O–H groups. The peaks at ~2500 cm^{-1} were assigned to the stretching and bending vibrations of C–H groups. The bending of the aromatic C=C groups could be also observed at 1490–1650 cm^{-1}. The sharp peaks at around 1343 cm^{-1} and 1090 cm^{-1} could be assigned to the stretching vibrations B–O and C–B groups (Figure 6C).[33,34]

Antibacterial Activity of Surface Functionalized CuONPs against *E.coli*. We examined the antibacterial activity of CuONPs surface functionalized with GLYMO and 4-HPBA on *E.coli* at pH 6. Although the bare CuONPs are cationic below pH 9, their functionalization with GLYMO resulted in weakly negatively charged CuONPs/GLYMO. Further functionalization with 4-HPBA also yielded negatively charged CuONPs/GLYMO/4-HPBA. The *E.coli* cells were extracted from the growth media and redispersed in deionized water and aliquots of this *E. coli* cultures were incubated with fixed concentration of the nanoparticles (i) under UV light, (ii) under visible light and (iii) in dark conditions.

The *E.coli* culture was incubated with CuONPs at different particle concentrations (0, 5, 10, 15, 20 and 25 µg mL^{-1}) for various durations (10 minutes, 1 hour and 6 hours). The viability of *E.coli* after this treatment in dark, visible and UV light conditions is showed in Figure 7 at various incubation times. It was noticed that immediately after exposure (10 minutes), the fraction of viable *E.coli* declined with in the presence of bare CuONPs and CuONPs/GLYMO/4-HPBA concentrations over 5 µg mL^{-1}. After 1 hour of such treatment in dark, visible light and UV light conditions, the viability of *E.coli* in the presence of nanoparticles was further reduced. After 6 hours incubation with 5-25 µg mL^{-1} CuONPs/GLYMO/4-HPBA, all *E.coli* lost completely their viability. Figures 7A, 7B and 7C show that the CuONPs had excellent antibacterial activity towards *E. coli*. There are many various mechanisms discussed in the literature about how CuONPs kill *E.coli* and their antibacterial action might be a mixture of all of them. One mechanism is based on the photoactive nature of these nanoparticles which in the presence of oxygen from air and visible or UV light, form reactive oxygen species (ROS) which are free radicals and lead to peroxidation of lipids from the bacterial cell membrane. [2,3,5,35]

The cell wall of *E.coli* is negatively charged while the un-functionalized (bare) CuONPs is positively charged (below pH 9). Therefore, the un-functionalized CuONPs were able to electrostatically adhere on the bacterial cell surface which led to damage of their cell membrane. When the free CuONPs attach to the cell, the ROS created locally can interact directly with the cell organelles which can amplify the cell damage. The ROS generation begins of a chain of free radical reactions inside the bacteria. Lipid peroxidation is a type of oxidative stress for the bacteria, which leads to its deactivation.

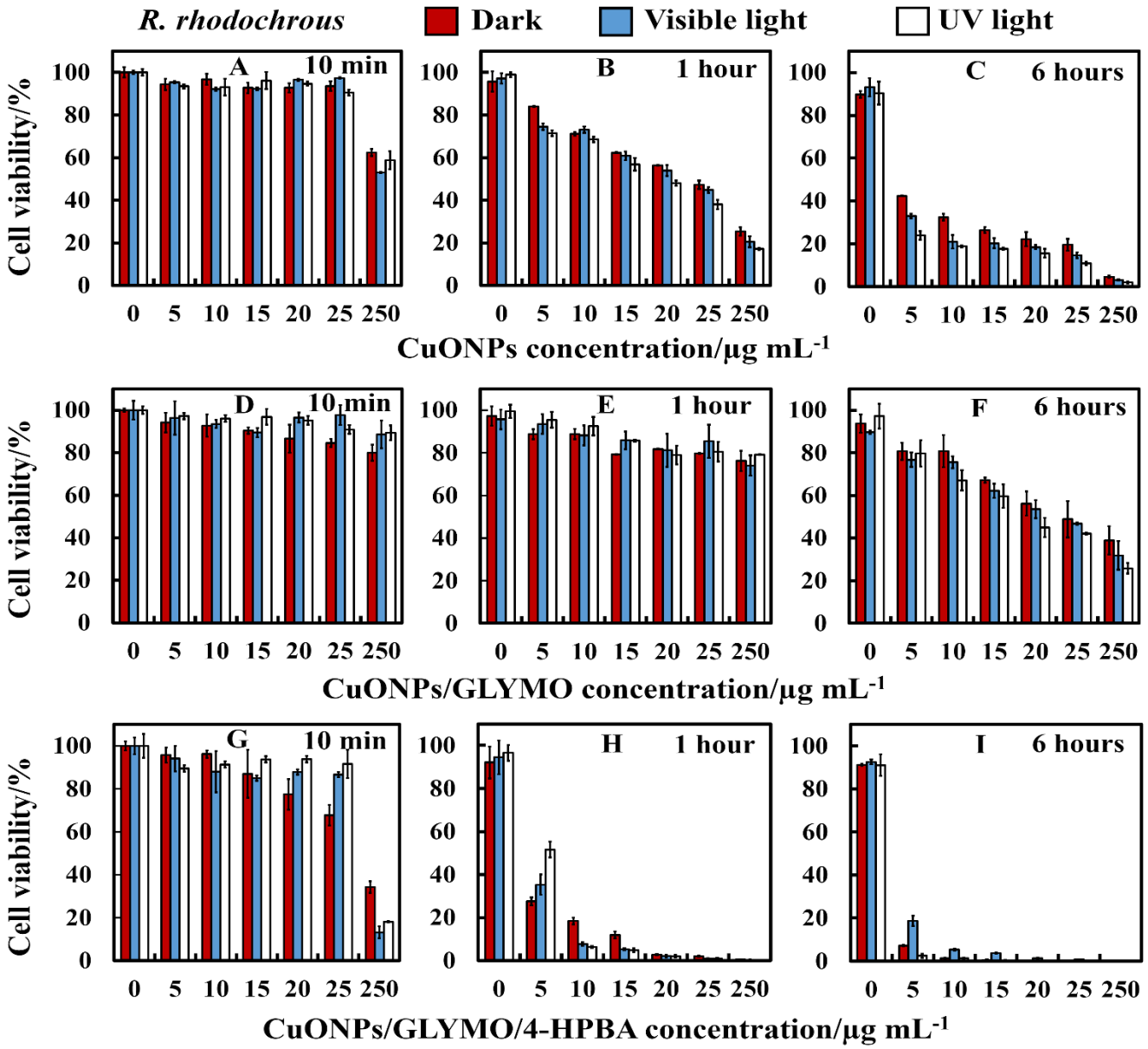

Figure 10. Cell viability of *R. rhodochrous* upon incubation of bare and surface functionalized of CuONPs of different particle concentrations (0, 5, 10, 15, 20, 25 and 250 µg mL^{-1}) in dark, visible and UV light conditions. The *R. rhodochrous* cells were incubated with: (A-C) bare CuONPs; (D-F) CuONPs/GLYMO and (G-I) CuONPs/GLYMO/4-HPBA at 10 min, 1 hour and 6 hours exposure times.

However, Figure 7 shows that the antibacterial activity of 25 µg mL^{-1} CuONPs towards *E.coli* under UV light for 1 hour is slightly higher than that under dark conditions. This suggests that the ROS generation under UV light has only a minor effect on the antibacterial action of CuONPs.

Another possible antimicrobial mechanism is the release of free Cu^{2+} ions from the CuONPs which may interfere with the cell membrane proteins. However, the concentration of free Cu^{2+} ions in the aqueous solution around the CuONPs is negligible due to its very small solubility. The values of the CuO solubility varies with pH but in pure water it is approximately 3×10^{-5} M. [36] This is not sufficient to explain the antimicrobial effect of CuONPs, which increases with their concentration, while the CuO solubility is constant at fixed pH and temperature).Our working hypothesis is that the strong antimicrobial action can be explained by the direct attraction of the cationic CuONPs with the anionic bacterial cell walls. As CuONPs are aggregates of rough surface, a likely explanation is that their adhesion to the membrane causes its rupture and this is the main contributing factor to the cell death – see below.

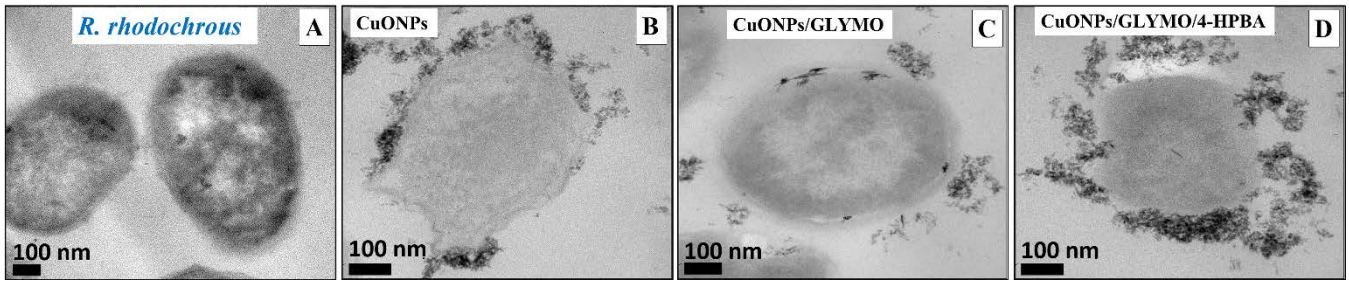

Figure 11. TEM images of *R. rhodochrous* after being incubated for 6 hours into 25 µg mL^{-1} bare and surface functionalized of CuONPs: (A) an untreated sample without CuONPs (B) *R. rhodochrous* incubated with CuONPs (C) *R. rhodochrous* incubated with CuONPs/GLYMO (D) *R. rhodochrous* incubated with CuONPs/GLYMO/4-HPBA.

We also found that the antibacterial effect of CuONPs/GLYMO (Figure 7D, 7E and 7F) is lower than the one of the bare CuONPs and CuONPs/GLYMO/4-HPBA. Note that CuONP/GLYMO are anionic at this pH and therefore lack electrostatic adhesion to the bacterial cell walls. Nevertheless, the introduction of a secondary functionalization of these anionic nanoparticles by conjugation of 4-HPBA made the produced CuONPs/GLYMO/4-HPBA much more effective against *E.coli* than the bare CuONPs. The later effect can be seen in Figure 7G, 7H and 7I. It is interesting that at lower CuONPs/GLYMO/4-HPBA concentrations (5 µg mL^{-1}) these anionic particles are several times more effective than the bare CuONPs and CuONPs/GLYMO irrespectively of the time of exposure in dark, visible or UV light conditions. These results require some discussion with respect to the possible factors that may contribute to the antibacterial activity of the CuONPs/GLYMO/4-HPBA. It has been shown that ligands with BA-functionality can covalently bind with diol compounds, like nucleotides, glycate-protein and saccharide.[22, 23, 37] Note that despite their negative surface charge, the anionic nanoparticles CuONPs/GLYMO/4-HPBA are showing a very significant antibacterial effect on *E.coli* even at lower particle concentrations than the bare CuONPs due to their covalent binding to the bacterial membrane. *E. coli* is surrounded by an outer membrane containing lipopolysaccharides (LPSs) with many diol-groups.[37-40] The strong (covalent) interactions between the boronic acid terminal group of the CuONPs/GLYMO/4-HPBA particles and the diol-groups from the LPS layer leads to the particle build-up on their cell membranes. In contrast, the adhesion of the bare CuONPs to the bacterial cell membrane is largely driven by electrostatic interactions while the CuONPs/GLYMO/4-HPBA bind to the surface saccharides through formation of boronic ester (see Figure 1). There are many examples in the literature where this effect has been utilized for sensing sugars[35,37, 41-42] but to our best knowledge this is the first time this idea is applied for antibacterial nanoparticle attachment to their targets. Direct CFU/mL measurements (see Figure S8 and S9 and Tables S1 and S2, ESI) also confirm the same trends for the effect of the CuONPs/GLYMO/4-HPBA compared to CuONPs for both *E.coli* and *R. rhodochrous*. Figures S10 and S11 show the reduction of the CuONPs/GLYMO/4-HPBA required to achieve the same antibacterial effect as CuONPs for these bacteria.

The *E.coli* samples were sectioned and imaged with SEM and TEM as described in the methods section. Figure 8 and Figure 9 show TEM and SEM images of *E. coli* cells after incubation with CuONPs functionalized with GLYMO and 4-HPBA for up to 6 hours. The images clearly show the adherent layer of nanoparticles which bind to the bacteria. The result was also confirmed via EDX chart of *E.coli* with CuONPs which revealed the presence of Cu on the external part of the *E.coli* surface (Figure S6, ESI).

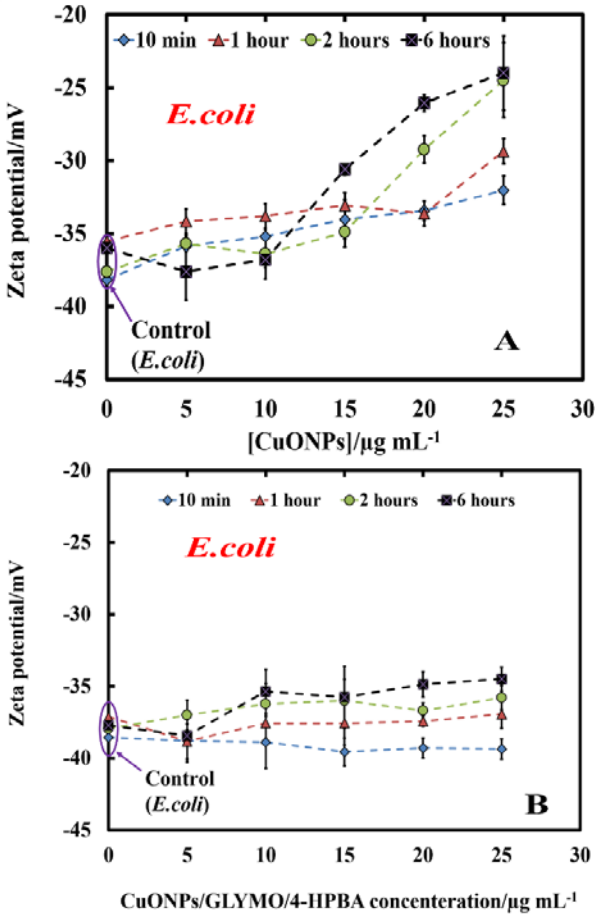

Figure 12. The zeta potential of *E. coli* in aqueous suspensions treated with various concentration of (A) bare CuONPs and (B) CuONPs/GLYMO/4-HPBA at various exposure times. Error bars indicate standard deviations of means.

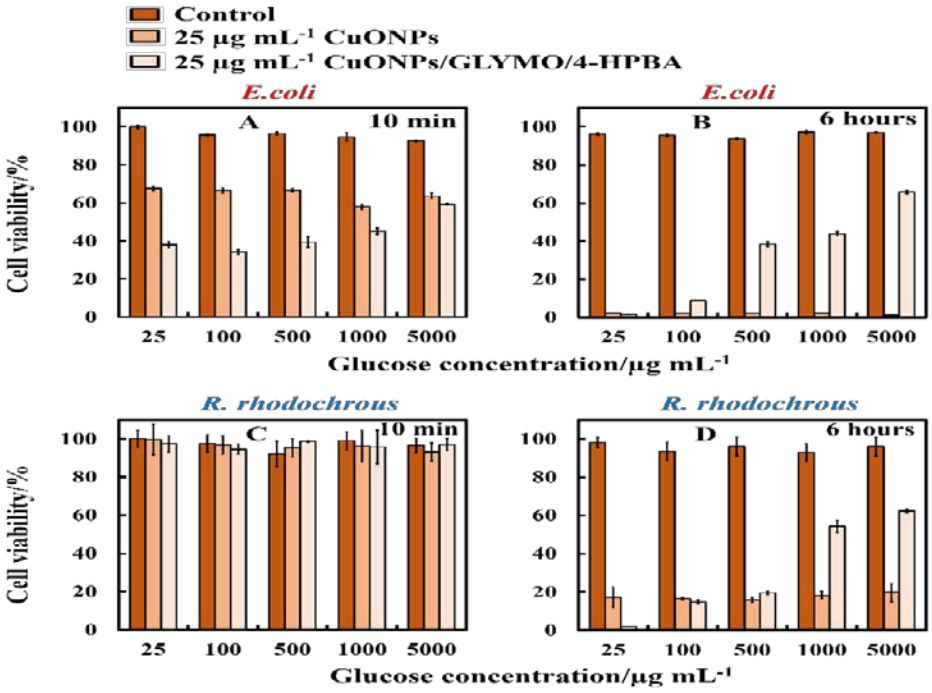

Figure 13. Bacterial cell viability after incubation as a function of nanoparticle concentration for 6 hours at various glucose concentrations (A and B) *E.coli* and (C and D) *R.rhodochrous*.

The occasional build-up of more than one layer of CuONPs/GLYMO/4-HPBA particles on the bacteria can also be a result of partial particle aggregation before they bind to the bacterial cell wall. The zeta-potential of the CuONPs is low by magnitude and such partial particle coagulation may take place at various stages of the sample preparation. However, the CuONPs/GLYMO/4-HPBA particles adhere to the negatively charged bacterial cell walls by covalent interactions despite their negative zeta potentials as they dominate the weaker electrostatic repulsion. We confirmed the result by performing EDX on sectioned *E. coli* and compared between bare CuONPs and 4-HPBA functionalized CuONPs which showed presence of Cu on the outer part of the cell membrane as CuONPs/GLYMO/4-HPBA much higher than the bare CuONPs ones as shown in Figure S13. Our results show higher Cu concentration on the bacteria outer cell wall for the functionalized CuONPs compared with the bare ones.

Antibacterial Properties of HPBA-Surface Functionalized CuONPs on *R. rhodochrous*. We also tested the antibacterial properties of the HPBA-modified CuONPs against Gram-positive bacteria. Figure 10 presents the antibacterial assay of *R. rhodochrous* where the control samples of untreated bacteria were compared with the ones treated with bare CuONPs, CuONPs/GLYMO and CuONPs/GLYMO/4-HPBA. Note that the cationic bare CuONPs are showing an antibacterial effect on *R. rhodochrous* even at moderate CuONPs concentrations (Figure 10B). We discovered that even at very low concentrations of CuONPs/GLYMO/4-HPBA they are several times more effective against *R. rhodochrous* (Figures 10H and 10I) than the bare CuONPs (Figure 10B and 10C) and CuONPs/GLYMO (Figure 10E and 10F). A strong effect of the bare CuONPs on *R. rhodochrous* viability was observed only after 6 hours of exposure time (Figure 10C). The charge of the bare CuONPs is an important factor to interact with *R. rhodochrous* membranes, which contribute to their high antibacterial activity.

Note that for exposure times up to 10 minutes and 1 hour (Figure 10D and E), no measurable change in the *R. rhodochrous* viability was detected for CuONPs/GLYMO even at high particle concentrations. This also confirms that potential release of Cu^{2+} ions is not the main factor in the antibacterial activity of these particles, as CuONPs/GLYMO would support the similar concentration of Cu^{2+} as the bare CuONPs. We also did not see a significant difference between the samples kept in dark, visible or in UV light conditions at the same CuONPs/GLYMO concentration. TEM imaging shows that the surfaces of *R. rhodochrous* cells accumulate a significant number of deposited nanoparticles after treatment for 6 hours with bare CuONPs (Figure 11B) and CuONPs/GLYMO/4-HPBA nanocomposites (Figure 11D). In contrast, the untreated (Figure 11A) and CuONPs/GLYMO treated *R. rhodochrous* (Figure 11C) show smooth and intact *R. rhodochrous* cell membranes.

An additional confirmation for the mechanism of attachment of the CuONPs/GLYMO/4-HPBA to bacterial cells is presented in Figure 12, where we compared the zeta-potential of *E. coli* after being treated with bare CuONPs and CuONPs/GLYMO/4-HPBA of different particle concentrations. Note that when the bacterial cells are treated with bare CuONPs, which are cationic at neutral pH, the zeta potential of the bacteria is reduced by

absolute value (Figure 12A) due to the partial deposition of the cationic CuONPs on the negatively charged bacterial cell wall.

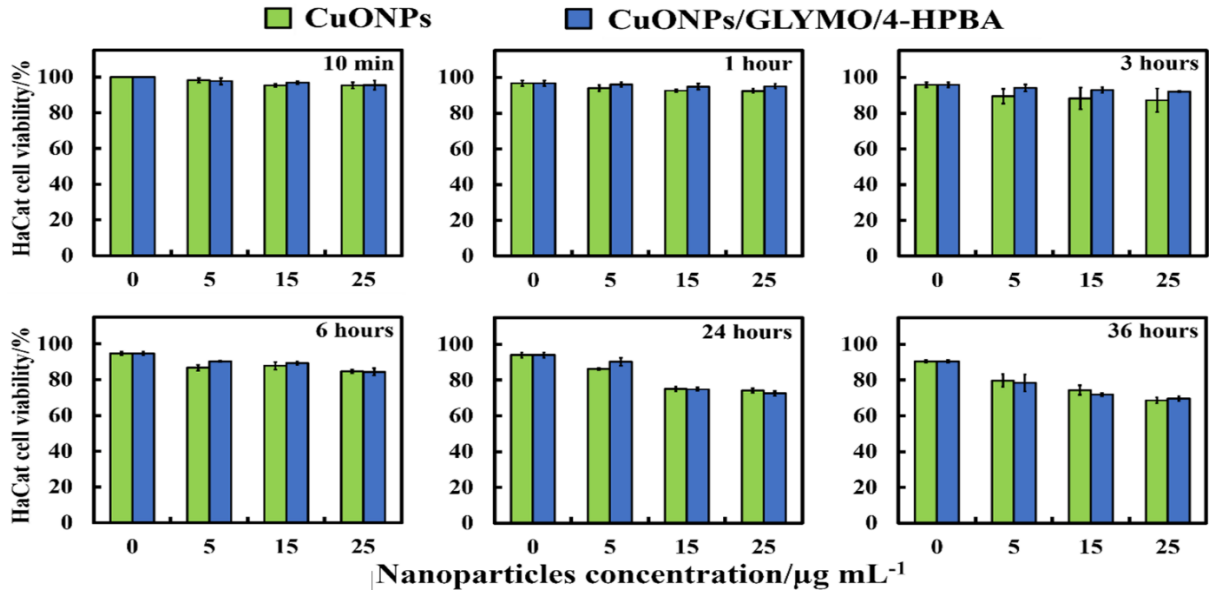

Figure 14. HaCaT cell viability after incubation as a function of nanoparticle concentration for up to 36 hours at with bare CuONPs and CuONPs/GLYMO/4-HPBA.

However, the incubation of the bacterial cells with CuONPs/GLYMO/4-HPBA does not incur measurable change in their zeta-potential despite their adsorption on the bacterial cell wall (Figure 12B). This is an additional confirmation that the attachment of the CuONPs/GLYMO/4-HPBA to the bacteria is not electrostatic and as Figures 10 and 11 indicate, the BA-functionalized CuONPs bind to the bacteria despite their negative surface charge. This result is easy to understand as the CuONPs/GLYMO/4-HPBA particles are anionic. SEM and TEM images (Figures 8 and 9) confirm the particle deposition of the *E.coli* outer membrane. These results suggest that the 4-HPBA functional group in the modified CuONPs/GLYMO/4-HPBA particles has a significant role in promoting adhesion to the *R. rhodochrous* membranes. The strong covalent attachment of the CuONPs/GLYMO/4-HPBA with the *R. rhodochrous* cell membrane is likely to be the main contributor towards the bacterial cell membrane disruption and damage which makes it a very efficient antibacterial agent.

Effect of the Presence of Glucose on the Antibacterial Activity of HPBA-Functionalized CuONPs towards *E.coli* and *R. rhodochrous* Figure 13 shows the antibacterial activity of the HPBA-surface functionalized CuONPs towards *E.coli* and *R. rhodochrous* at different concentrations of glucose and fixed nanoparticle concentration of 25 μg mL^{-1}. Note that all bacteria apparently lost their viability in the presence of bare CuONPs after 6 hours independently of the concentration of glucose in the solution. However, the bacteria viability in the presence of CuONPs/GLYMO/4-HPBA increased with increasing of the glucose concentration. A possible mechanism for this could be that in the presence of glucose the boronic acid functional groups of the CuONPs/GLYMO/4-HPBA nanoparticles bind to the free glucose in solution thus reducing the interaction between 4-HPBA terminal group and the bacterial membranes. This also confirms that the mechanism of attachment of the CuONPs/GLYMO/4-HPBA to the bacteria is based on binding to sugar groups.

Cytotoxicity of Bare and HPBA-Functionalized CuONPs on Human Keratinocytes. Figure 14 shows the cytotoxicity assay of CuONPs and CuONPs/GLYMO/HPBA on HaCaT cells for up to several hours of exposure. The results confirm that CuONPs/GLYMO/HPBA have negligible toxic effect on these cells while bare CuONPs have some low level of toxicity compared with the control sample. These results are obtained with particle concentrations where they are showing very strong antibacterial effect on *E.coli* and *R. rhodochrous* while leaving the keratinocyte cells unaffected. We took SEM images of dehydrated HaCaT cells after being treated with bare and HPBA-functionalized CuONPs and compared them with SEM images of the control ssample (no treatment). The results are presented in Figure S12. In both cases, we did not observe significantly different build-up of CuONPs on these images which does not allow directly to differentiate the mechanism of their potential cytotoxic action on keratinocytes. One possible explanation why the skin cells are unaffected by both the bare and the functionalized CuONPs could be that their membrane is easier to bend around the adhering rough nanoparticles and is less prone to dislocation and rupture than the rigid membranes of bacteria.[6] This result is reassuring that such antimicrobial particles can potentially find application in wound care formulations as an alternative to antimicrobial delivery vehicles.[43,44]

CONCLUSIONS

In summary, we have developed a novel type of modified CuONPs which have been functionalized with GLYMO and 4-HPBA (CuONPs/GLYMO/4-HPBA) to produce an antibacterial agent of much higher efficiency than bare CuONPs. This novel coating with boronic acid functionality

allows the antimicrobial particles to form covalent bonds with the diol groups from carbohydrates expressed on the cell wall of both Gram-positive and Gram–negative bacteria. We demonstrate the profound differences in the surface properties of the bare CuONPs and the CuONPs/GLYMO/4-HPBA particles which at neutral pH have different surface charge. The zeta potential of non-functionalized CuONPs, GLYMO-functionalized CuONPs and 4-HPBA-functionalized CuONPs was +37 mV, -3 mV and -10 mV, respectively. It was found that both nanoparticles showed opposite surface charge in the aqueous solution at pH 6 as their zeta potential decreased from +37 mV to -10 mV. Our antibacterial assays showed that the anionic nanoparticles as CuONPs/GLYMO/4-HPBA have much higher antibacterial action than the cationic ones non-functionalized CuONPs for both Gram-positive and Gram-negative bacteria. This is explained by the strong adhesion of the anionic particles CuONPs/GLYMO/4-HPBA to the cell walls due to their covalent interactions between the terminal 4-Hydroxyphenylboronic acid group and carbohydrates on the cell surface. SEM and TEM images of *R. rhodochrous* and *E.coli* exposed to 4-HPBA functionalized CuONPs confirmed the formation of a significant build-up of these nanoparticles on the bacterial cell outer membrane. Control experiments proved that the binding ability of the modified CuONPs/GLYMO/4-HPBA to bacteria can be adjusted and reversed by adding glucose in the media which engages the boronic acid groups of the CuONPs surface and lessens their ability to attach to bacteria. This effect allows direct control over their antimicrobial action. Preliminary experiments of incubation of the HPBA-functionalized CuONPs with human keratinocytes showed no measurable cytotoxicity. In general, we envisage that this type of functionality can be successfully applied to a range of inorganic nanoparticles, as ZnONPs, TiO_2NPs, Ag_2ONPs, Cu_2ONPs and others which would lead to fabrication of superior antimicrobial agents at significantly lower particle concentration.

AUTHOR INFORMATION

Corresponding Author

* Phone +44 1482 465660. Email: V.N.Paunov@hull.ac.uk

ORCID

Ahmed F. Halbus: 0000-0001-9060-7073
Tommy S. Horozov: 0000-0001-8818-3750
Vesselin N. Paunov: 0000-0001-6878-1681

Author Contributions

The manuscript was written through contributions of all authors. All authors have given approval to the final version of the manuscript.

Funding Sources

A.F.H acknowledge funding of this work from the Higher Committee for Education Development of Iraq and the University of Babylon, Iraq.

ACKNOWLEDGMENTS

A.F.H. thanks the Iraqi Government, the Higher Committee for Education Development of Iraq and the University of Babylon, Iraq for the financial support for his PhD study during the work on this project. The authors appreciated the technical help from Tony Sinclair and Ann Lowry at the University of Hull Microscopy Suite with the SEM and TEM sample preparation and imaging. We also thank Zahraa Al-Mashaykhi for her help with FTIR measurements.

ASSOCIATED CONTENT

In the enclosed electronic supplementary information (ESI) we present the following additional data: (i) The Schematics of the synthesis method of CuONPs; (ii) FTIR analysis of CuONPs calcined at various Temperatures; (iii) XRD pattern of CuONPs annealed at different temperatures; (iv) Effect of the annealing temperature on the particles size and zeta potential of the CuONPs; (v) EDX Diagram of E.coli cells with bare CuONPs (vi) Stability of the zeta-potential of bare and functionalized CuONPs; (vi) CFU assessment of the viability of E. Coli and R. rhodochrous after treatment with bare and functionalized CuONPs; (vi) Antimicrobial efficiency of the bare and HPBA-functionalized CuONPs; (vii) SEM images of HaCaT cells treated with bare- and HPBA-functionalized CuONPs; (viii) EDX diagrams of the outer surface of E. coli treated with bare-andHPBA-functionalized CuONPs

REFERENCES

(1) Mi, G.; Shi, D.; Wang, M.; Webster, T.J.; Reducing Bacterial Infections and Biofilm Formation Using Nanoparticles and Nanostructured Antibacterial Surfaces, *Adv. Healthcare Mater*., **2018**, *7*, 1800103.

(2) Halbus, A. F.; Horozov, T. S.; Paunov, V. N. Colloid Particle Formulations for Antimicrobial Applications. *Adv. Colloid Interface Sci.* **2017,** *249*, 134-148.

(3) Yuan, P.; Ding, X.; Yang, Y.Y.; Xu, Q.-H.; Metal Nanoparticles for Diagnosis and Therapy of Bacterial Infection, *Adv. Healthcare Mater*., **2018**, 7, 1701392.

(4) Alpaslan, E.; Geilich, B.M.; Yazici, H.; Webster, T.J., pH-Controlled Cerium Oxide Nanoparticle Inhibition of Both Gram-Positive and Gram-Negative Bacteria Growth, *Sci. Rep.*, **2017**, *7*, 45859.1-12.

(5) Seil, J.T.; Webster, T.J.; Antimicrobial Applications of Nanotechnology: Methods and Literature, *Int. J. Nanomedicine*. **2012**, *7*, 2767–2781.

(6) Penders, J.; Stolzoff, M.; Hickey, D.J.; Andersson, M.; Webster, T.J., Shape-Dependent Antibacterial Effects of Non-Cytotoxic Gold Nanoparticles, *Int. J. Nanomedicine*, **2017**, *12*, 2457–2468.

(7) Grigore, M. E.; Biscu, E. R.; Holban, A. M.; Gestal, M. C.; Grumezescu, A. M. Methods of Synthesis, Properties and Biomedical Applications of CuO Nanoparticles. *Pharmaceuticals* **2016,** *9*, 75.

(8) Ahamed, M.; Alhadlaq, H. A.; Khan, M.; Karuppiah, P.; Al-Dhabi, N. A. Synthesis, Characterization, and Antimicrobial Activity of Copper Oxide Nanoparticles. *J. Nanomater*. **2014,** *2014*, 1-4.

(9) Lazary, A.; Weinberg, I.; Vatine, J.-J.; Jefidoff, A.; Bardenstein, R.; Borkow, G.; Ohana, N. Reduction of Healthcare-Associated Infections in a Long-Term Care Brain Injury Ward By Replacing Regular Linens With Biocidal Copper Oxide Impregnated Linens. *Int. J. Infect. Dis.* **2014,** *24*, 23-29.

(10) sani Usman, M. Synthesis, Characterization, and Antimicrobial Properties of Copper Nanoparticles. *Int. J. Nanomedicine* **2013,** *8*, 4467-4479.

(11) Mahapatra, O.; Bhagat, M.; Gopalakrishnan, C.; Arunachalam, K. D. Ultrafine Dispersed CuO Nanoparticles and their Antibacterial Activity. *J Exp Nanosci*. **2008,** *3*, 185-193.

(12) Katwal, R.; Kaur, H.; Sharma, G.; Naushad, M.; Pathania, D. Electrochemical Synthesized Copper Oxide Nanoparticles for Enhanced Photocatalytic and Antimicrobial Activity. *Ind. Eng. Chem.* **2015,** *31*, 173-184.

(13) Azam, A.; Ahmed, A. S.; Oves, M.; Khan, M.; Memic, A. Size-Dependent Antimicrobial Properties of CuO Nanoparticles Against Gram-Positive and-Negative Bacterial Strains. *Int. J. Nanomed* **2012,** *7*, 3527-3535.

(14) De Silva, A. P.; Gunaratne, H. N.; Gunnlaugsson, T.; Huxley, A. J.; McCoy, C. P.; Rademacher, J. T.; Rice, T. E. Signaling Recognition Events with Fluorescent Sensors and Switches. *Chem. Rev*. **1997,** *97*, 1515-1566.

(15) Lacina, K.; Skládal, P.; James, T. D. Boronic Acids for Sensing and other Applications-A Mini-Review of Papers Published in 2013. *Chem. Cent. J*. **2014,** *8*, 1-17.

(16) Trippier, P. C.; McGuigan, C. Boronic Acids in Medicinal Chemistry: Anticancer, Antibacterial and Antiviral Applications. *MedChemComm.* **2010,** *1*, 183-198.

(17) Yan, J.; Springsteen, G.; Deeter, S.; Wang, B. The Relationship Among pKa, pH, and Binding Constants in the Interactions Between Boronic Acids and Diols—it is not as Simple as it Appears. *Tetrahedron* **2004,** *60*, 11205-11209.

(18) Kuzimenkova, M. V.; Ivanov, A. E.; Thammakhet, C.; Mikhalovska, L. I.; Galaev, I. Y.; Thavarungkul, P.; Kanatharana, P.; Mattiasson, B. Optical Responses, Permeability and Diol-Specific Reactivity of Thin Polyacrylamide Gels Containing Immobilized Phenylboronic Acid. *Polymer* **2008,** *49*, 1444-1454.

(19) Lau, O.-W.; Shao, B.; Lee, M. T. Affinity Mass Sensors: Determination of Fructose. *Anal. Chim. Acta* **2000,** *403*, 49-56.

(20) Ertl, P.; Mikkelsen, S. R. Electrochemical Biosensor Array for the Identification of Microorganisms Based on Lectin−Lipopolysaccharide Recognition. *Anal. Chem.* **2001,** *73*, 4241-4248.

(21) Wannapob, R.; Kanatharana, P.; Limbut, W.; Numnuam, A.; Asawatreratanakul, P.; Thammakhet, C.; Thavarungkul, P. Affinity Sensor Using 3-aminophenylboronic Acid for Bacteria Detection. *Biosens. Bioelectron.* **2010,** *26*, 357-364.

(22) Liu, S.; Wollenberger, U.; Halámek, J.; Leupold, E.; Stöcklein, W.; Warsinke, A.; Scheller, F. W. Affinity Interactions Between Phenylboronic Acid-Carrying Self-Assembled Monolayers and Flavin Adenine Dinucleotide or Horseradish Peroxidase. *Chem. Eur.J*. **2005,** *11*, 4239-4246.

(23) Elmas, B.; Onur, M.; Şenel, S.; Tuncel, A. Temperature Controlled RNA Isolation by N-Isopropylacrylamide–Vinylphenyl Boronic Acid Copolymer latex. *Colloid. Polym. Sci.* **2002,** *280*, 1137-1146.

(24) DiCesare, N.; Lakowicz, J. R. Evaluation of two Synthetic Glucose Probes for Fluorescence-Lifetime-Based Sensing. *Anal. Biochem.* **2001,** *294*, 154-160.

(25) Pandey, V.; Mishra, G.; Verma, S.; Wan, M.; Yadav, R. Synthesis and Ultrasonic Investigations of CuO-PVA Nanofluid. *Mater. Sci. Appl*. **2012,** *3*, 664-668.

(26) Grasset, F.; Saito, N.; Li, D.; Park, D.; Sakaguchi, I.; Ohashi, N.; Haneda, H.; Roisnel, T.; Mornet, S.; Duguet, E. Surface Modification of Zinc Oxide Nanoparticles by Aminopropyltriethoxysilane. *J. Alloys Compd*. **2003,** *360*, 298-311.

(27) Zhang, D.; Thompson, K.L.; Pelton, R.; Armes, S.P.; Controlling Deposition and Release of Polyol-Stabilized Latex on Boronic Acid-Derivatized Cellulose, *Langmuir*, **2010**, 26, 17237–17241.

(28) Pelton, R.; Zhang, D.; Thompson, K.L.; Armes, S.P.; Borate Binding to Polyol-Stabilized Latex, *Langmuir*, **2011**, 27, 2118–2123.

(29) Cunningham, V. J.; Alswieleh, A. M.; Thompson, K. L.; Williams, M.; Leggett, G. J.; Armes, S. P.; Musa, O. M. Poly(glycerol monomethacrylate)–Poly(benzyl methacrylate) Diblock Copolymer Nanoparticles via RAFT Emulsion Polymerization: Synthesis, Characterization, and Interfacial Activity. *Macromolecules* **2014,** *47*, 5613-5623.

(30) Manimaran, R.; Palaniradja, K.; Alagumurthi, N.; Sendhilnathan, S.; Hussain, J. Preparation and Characterization of Copper Oxide Nanofluid for Heat Transfer Applications. *Appl. Nanosci.* **2014,** *4*, 163-167.

(31) Luna, I. Z.; Hilary, L. N.; Chowdhury, A. S.; Gafur, M.; Khan, N.; Khan, R. A. Preparation and Characterization of Copper Oxide Nanoparticles Synthesized via Chemical Precipitation Method. *OALib. J.* **2015,** *2*, 1-8.

(32) Premazu, P. T.; Stabilization of Rutile TiO_2 Nanoparticles with Glymo in Polyacrylic Clear Coating. *Mater. Tehnol.* **2012,** *46*, 19-24.

(33) Guo, Y.; Chen, Y.; Cao, F.; Wang, L.; Wang, Z.; Leng, Y. Hydrothermal Synthesis of Nitrogen and Boron Doped Carbon Quantum Dots with Yellow-Green Emission for Sensing Cr (VI), Anti-Counterfeiting and Cell Imaging. *RSC Adv*. **2017,** *7*, 48386-48393.

(34) Arslan, M.; Kiskan, B.; Yagci, Y. Recycling and Self-Healing of Polybenzoxazines with Dynamic Sulfide Linkages. *Sci. Rep.* **2017,** *7*, 5207.

(35) Al-Awady, M. J.; Greenway, G. M.; Paunov, V. N. Nanotoxicity of Polyelectrolyte-Functionalized Titania Nanoparticles Towards Microalgae and Yeast: Role of the Particle Concentration, Size and Surface Charge. *RSC Adv*. **2015,** *5*, 37044-37059.

(36) Murray, J.V.; Cloke, J.B.; The Solubility of Cupric Oxide in Alkali and the Second Dissociation Constant of Cupric Acid. The Analysis of Very Small Amounts of Copper, *J. Am. Chem. Soc.*, **1936**, 58, 2009–2014.

(37) Amin, R.; Elfeky, S. A. Fluorescent Sensor for Bacterial Recognition. *Spectrochim. Acta A Mol. Biomol. Spectrosc.* **2013,** *108*, 338-341.

(38) Tümer, M.; Köksal, H.; Sener, M. K.; Serin, S. Antimicrobial Activity Studies of the Binuclear Metal Complexes Derived from Tridentate Schiff Base Ligands. *Transition Met. Chem.* **1999,** *24*, 414-420.

(39) Imran, M.; Iqbal, J.; Iqbal, S.; Ijaz, N. In Vitro Antibacterial Studies of Ciprofloxacin-Imines and their Complexes with Cu (II), Ni (II), Co (II), and Zn (II). *Turk. J. Biol.* **2007,** *31*, 67-72.

(40) Maillard, A. P. F.; Dalmasso, P. R.; de Mishima, B. A. L.; Hollmann, A. Interaction of Green Silver Nanoparticles with Model Membranes: Possible Role in the Antibacterial Activity. *Colloids Surf. B Biointerfaces* **2018,** *171*, 320-326.

(41) Wiskur, S. L.; Lavigne, J. J.; Ait-Haddou, H.; Lynch, V.; Chiu, Y. H.; Canary, J. W.; Anslyn, E. V. p K a Values and Geometries of Secondary and Tertiary Amines Complexed to Boronic Acids Implications for Sensor Design. *Org. Lett.* **2001,** *3*, 1311-1314.

(42) Hartley, J. H.; James, T. D.; Ward, C. J. Synthetic Receptors. *J. Chem. Soc., Perkin Trans. 1* **2000,** (19), 3155-3184.

(43) Al-Awady, M. J.; Fauchet, A.; Greenway, G. M.; Paunov, V. N. Enhanced Antimicrobial Effect of Berberine in Nanogel Carriers with Cationic Surface Functionality. *J. Mater. Chem. B* **2017,** *5*, 7885-7897.

(44) Al-Awady, M. J.; Weldrick, P. J.; Hardman, M. J.; Greenway, G. M.; Paunov, V. N. Amplified Antimicrobial Action of Chlorhexidine Encapsulated in PDAC-Functionalized Acrylate Copolymer Nanogel Carriers. *Mater. Chem. Front.* **2018,** *2*, 2032-2044.

(45) Lowry, G.V.; Gregory, K.B.; Apte, S.C.; Lead, J.R.; Transformations of Nanomaterials in the Environment. *Environ. Sci. Technol*. **2012**, 46, 6893-6899.

(46) Líbalová, H.; Costa, P. M.; Olsson, M.; Farcal, L.; Ortelli, S.; Blosi, M.; Topinka, J.; Costa, A. L.; Fadeel, B.; Toxicity of Surface-Modified Copper Oxide Nanoparticles in a Mouse Macrophage Cell Line: Interplay of Particles, Surface Coating and Particle Dissolution. *Chemosphere*. **2018**, 196, 482-493.

(47) Chen, K.L.; Bothun, G.D.; Nanoparticles Meet Cell Membranes: Probing Nonspecific Interactions Using Model Membranes. *Environ. Sci. Technol.* **2014**, 48, 873-880.

(48) Perreault, F.; Oukarroum, A.; Melegari, S.P.; Matias, W.G.; Popovic, R.; Polymer Coating of Copper Oxide Nanoparticles Increase Nanoparticles Uptake and Toxicity in the Green Alga Chlamydomonas Reinhardtii. *Chemosphere*. **2012**, 87, 1388-1394.

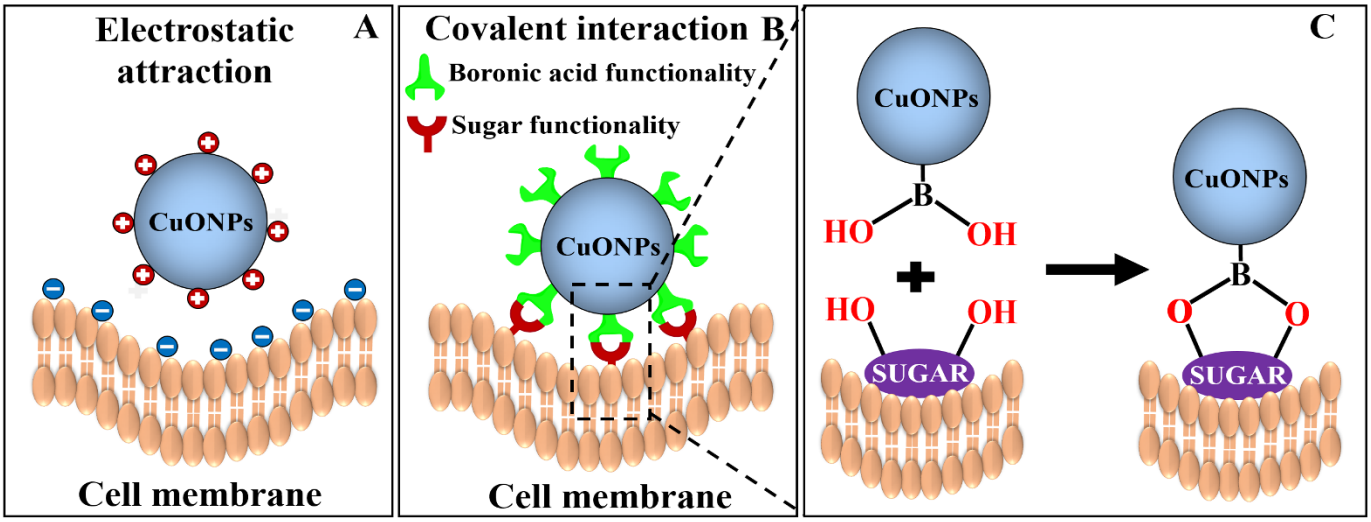
Electrostatic attraction
A
CuONPs
Cell membrane
Covalent interaction B
Boronic acid functionality
Sugar functionality
CuONPs
Cell membrane
C
CuONPs
B
HO
OH
HO
OH
SUGAR
CuONPs
B
O
O
SUGAR